

Projected SO(5) models

Shou-Cheng Zhang and Jiang-Ping Hu

Department of Physics, Stanford University, Stanford, California 94305

Enrico Arrigoni and Werner Hanke

Institut für Theoretische Physik, Universität Würzburg, Am Hubland, D-97074 Würzburg, Federal Republic of Germany

Assa Auerbach

Department of Physics, Technion, Haifa 32000, Israel

(Received 16 April 1999)

We construct a class of projected SO(5) models where the Gutzwiller constraint of no-double-occupancy is implemented exactly. We introduce the concept of projected SO(5) symmetry where all static correlation functions are exactly SO(5) symmetric and discuss the signature of the projected SO(5) symmetry in dynamical correlation functions. We show that this class of projected SO(5) models can give a realistic description of the global phase diagram of the high- T_c superconductors and account for many of their physical properties.
[S0163-1829(99)12241-0]

I. INTRODUCTION

Recently, a unified theory of antiferromagnetism (AF) and superconductivity (SC) has been proposed for the high- T_c cuprates.¹ This theory is based on the SO(5) symmetry between AF and SC, and offers a unified description of the global phase diagram for this class of materials. While the theory was originally proposed as a effective field theory description, it was soon realized that the SO(5) symmetry could be implemented exactly at a microscopic level,²⁻⁶ and it can also be checked numerically in common strongly correlated models such as the t - J model.⁷⁻⁹ While the phase diagram^{1,10-12} and collective excitations^{13,14} in the SC state derived from these SO(5) models bear strong resemblance to the high- T_c cuprates, and a number of experimental predictions have been made,¹⁵⁻¹⁹ the Mott insulating behavior at half-filling is a puzzling aspect which challenges the fundamental validity of the SO(5) models.²⁰⁻²³ To be more precise, the exact SO(5) symmetry requires collective charge two excitation at half-filling to have the same mass as the collective spin-wave excitations. This condition is clearly violated in a Mott insulating system where all charge excitations measured with respect to a particle-hole symmetric point have a large energy gap of few eV, while the spin-wave excitations are massless. In the original SO(5) proposal, it was pointed out that this situation is analogous to a easy-axis antiferromagnet in a external uniform field, and a SO(5) symmetry breaking term at half-filling was introduced in order to describe this asymmetric behavior between spin and charge. The chemical potential also introduces a SO(5) symmetry breaking term, however, it was shown that these two terms could compensate each other^{1,8} so that the *static potential* governing the SO(5) superspin could still be SO(5) symmetric.

Since the asymmetry between the charge and spin excitations at half-filling is of the order of the Coulomb energy scale U , the SO(5) symmetry breaking terms must also be of that order. Since there are various types of symmetry breaking terms, one might hope that their effects could partially

cancel each other to arrive at a qualitatively correct picture. However, this type of cancellation is very delicate, and approximate calculations could easily lead to erroneous conclusions. In particular, one is interested in which physical properties could exhibit SO(5) symmetric properties in the limit when the Coulomb gap is taken to infinity. For example, one could ask the following questions.

(1) One of the hallmarks of the SO(5) symmetry is not only the degeneracy between the AF and SC states at a given chemical potential, but the approximate degeneracy among all mix states interpolating between AF and SC, i.e., the independence of the ground-state energy on the superspin angle. What is the potential barrier separating the AF and SC states at their degeneracy point in the limit $U \rightarrow \infty$? If there is a large energy barrier in this limit, one would argue that the concept of SO(5) symmetry is not a useful one, at least not for quantitative calculations. On the other hand, if the potential barrier is finite and small in the $U \rightarrow \infty$ limit, the concept of a approximate SO(5) symmetry would be a useful one.

(2) Exact SO(5) symmetry predicts four massless collective modes. In the half-filled AF state, besides the two conventional massless spin-wave modes, the exact SO(5) symmetry predicts a massless doublet of π^\pm modes, with charge ± 2 . However, a Mott insulator has a large gap to all charge excitations. Therefore, it is clear that one of the π^\pm has to be projected out of the spectrum in the limit $U \rightarrow \infty$, say, the π^+ mode carrying charge $+2$. What happens to the rest of the Goldstone modes, the π^- mode carrying charge -2 and the π^α triplet mode of the SC state? In the $U \rightarrow \infty$ limit, can they all be simultaneously massless at the transition point between AF and SC? Since the pure SC state can only be reached with a finite doping concentration, is it possible that the Gutzwiller projection does not affect the π^α triplet mode of the SC state?

In order to address these questions, it is desirable to construct a low-energy effective theory without any parameters of the order of the Coulomb scale U . In this work, we construct a class of projected SO(5) models which treat the

Gutzwiller constraint exactly and locally on every site. We use this model to answer the physical questions posed above and show that the answers are affirmative. In the $U \rightarrow \infty$ limit, when the Gutzwiller constraint is implemented exactly, the ground-state energy can still be SO(5) symmetric and independent of the superspin direction. After projecting out the π^+ mode, all other Goldstone modes remain massless at the symmetric point. The dispersion relation of the collective modes bear the unique signature of the projected SO(5) symmetry. Furthermore, the π^α triplet modes of the pure SC states are unaffected by the Gutzwiller projection. These properties define the concept of a projected SO(5) symmetry [pSO(5)], whose properties and consequences we shall explore in this paper.

The fundamental quantity in the SO(5) theory is the locally defined five-component superspin vector $n_a(x) = (n_1, n_2, n_3, n_4, n_5)$ describing the local AF and SC order parameters, respectively. In the nonlinear σ model formalism, these are treated as mutually commuting coordinates and their dynamics is given by their conjugate momenta $p_a(x) = (p_1, p_2, p_3, p_4, p_5)$. The charge operator is the angular momentum in the $n_1 - n_5$ plane:

$$Q(x) = L_{15} = n_1 p_5 - n_5 p_1. \quad (1.1)$$

Implementing the Gutzwiller constraint corresponds to requiring

$$Q(x) \leq 0 \quad (1.2)$$

for every local SO(5) rotor. From Eqs. (1.1) and (1.2) and subsequent discussions, we shall see that the Gutzwiller projection in the SO(5) formalism corresponds to going from a fully symmetric SO(5) rotor model to a *chiral* SO(5) rotor model, where both the static potential of the individual rotors and the coupling between the rotors are still SO(5) symmetric, but the rotors are constrained to rotate only in one sense in the $n_1 - n_5$ plane, consistent with Eq. (1.2). This observation reveals a deep connection between the Gutzwiller projection and the lowest-Landau-level (LLL) projection in the fractional quantum Hall effect.²⁴ To be more precise, the Gutzwiller projection represented by Eqs. (1.1) and (1.2) is analogous to the LLL projection, where all states in the LLL have a definite sign of angular momentum. The LLL projection can be analytically implemented by separating the cyclotron degrees of freedom from the guiding center degrees of freedom, which amounts to changing the commuting property between the X and Y coordinates to a canonically conjugate commutation relation:

$$[X, Y] = i l_0, \quad (1.3)$$

where l_0 is the Landau length. Exploiting this analogy, we find that the original SO(5) model can be fully Gutzwiller projected without changing its form, if one imposes the simple quantization condition between the superconducting components of the superspin vector:

$$[n_1, n_5] = i/2. \quad (1.4)$$

In the symmetric SO(5) model, the wave function of the SO(5) rotors are functions of the local coordinates n_1 and n_5 , while the projected SO(5) model only depends on their holomorphic combination $z = n_1 - i n_5$ and is independent of

$$\begin{aligned} |\Omega\rangle &: \quad \left| \begin{smallmatrix} \uparrow \\ \uparrow \end{smallmatrix} \right\rangle - \left| \begin{smallmatrix} \downarrow \\ \downarrow \end{smallmatrix} \right\rangle \\ t_a |\Omega\rangle &: \quad \left| \begin{smallmatrix} \uparrow \\ \uparrow \end{smallmatrix} \right\rangle, \quad \left| \begin{smallmatrix} \uparrow \\ \downarrow \end{smallmatrix} \right\rangle + \left| \begin{smallmatrix} \downarrow \\ \uparrow \end{smallmatrix} \right\rangle, \quad \left| \begin{smallmatrix} \uparrow \\ \uparrow \end{smallmatrix} \right\rangle \\ t_h |\Omega\rangle &: \quad \left| \begin{smallmatrix} = \\ \uparrow \end{smallmatrix} \right\rangle \\ t_p |\Omega\rangle &: \quad \left| \begin{smallmatrix} \# \\ \# \end{smallmatrix} \right\rangle \end{aligned}$$

FIG. 1. Schematic representation of the singlet state, the triplet magnon states and the hole and particle pair states.

their antiholomorphic combination $\bar{z} = n_1 + i n_5$. This way, we arrive at a natural projection of the SO(5) model where the local Gutzwiller constraint is taken into account exactly, and the resulting model is free of the large Coulomb U parameter. Because the functional form of the symmetric SO(5) model remain the same and only the quantization condition is modified upon projection, many important properties associated with the SO(5) symmetry remain. The central hypothesis of the SO(5) theory is that this projected model is quantitatively accurate in describing both the static and dynamic properties of the high- T_c cuprates, and we shall compare the properties of this model with the phenomenology of the high- T_c systems.

II. CONSTRUCTION OF PROJECTED SO(5) MODELS

We begin with the symmetric SO(5) Hamiltonian defined on a lattice,

$$\begin{aligned} H = & \Delta \sum_x L_{ab}^2(x) - J \sum_{\langle xx' \rangle} n_a(x) n_a(x') \\ & + V \sum_{\langle xx' \rangle} L_{ab}(x) L_{ab}(x'), \end{aligned} \quad (2.1)$$

where $n_a(x)$ denotes the five-component superspin vector on a given site, and $L_{ab}(x)$ is the SO(5) symmetry generator,

$$L_{ab} = n_a p_b - n_b p_a \quad (2.2)$$

expressed here in terms of the superspin vector n_a and its canonically conjugate momenta p_a ,

$$[n_a, p_b] = i \delta_{ab}. \quad (2.3)$$

This lattice quantum nonlinear σ model can be rigorously derived as the low-energy limit of a microscopic SO(5) ladder model.^{5,6} On the ladder, the rung SO(5) singlet state is the vacuum $|\Omega\rangle$, from which the lowest SO(5) multiplet $|a\rangle = t_a^\dagger |\Omega\rangle$ is created by a quintet of Bose creation operators, which satisfy

$$[t_a, t_b^\dagger] = \delta_{ab}, \quad t_a |\Omega\rangle = 0. \quad (2.4)$$

Here, $a=2,3,4$ denote the triplet (magnon) states, and $a=1,5$ are the hole and particle pair states (see Fig. 1). The superspin coordinates are microscopically constructed using these lattice bosons,

$$n_a = \frac{1}{\sqrt{2}} (t_a + t_a^\dagger), \quad p_a = \frac{1}{i\sqrt{2}} (t_a - t_a^\dagger). \quad (2.5)$$

Due to their microscopic origin, these bosonic states are hard-core bosons, in the sense that one cannot define two of them on the same rung. The Δ term in Eq. (2.1) describes the

gap energy of the magnon and the pair states, the J term stands for the hopping and the spontaneous creation/destruction process of these states, and the V term describes their nearest-neighbor interaction. This quantum nonlinear σ model can in principle also be derived in higher dimensions from a microscopic SO(5) symmetric model,²⁻⁴ by introducing a superspin vector as a Hubbard-Stratonovich decoupling field, and integrate out the fermionic degrees of freedom in a gradient expansion. However, we shall proceed more heuristically here.²⁵ For a two-dimensional system, one can imagine that the quantum σ model Hamiltonian is obtained from a ‘‘block spin’’ type of coarse graining of the microscopic electron Hamiltonian, and is defined on a lattice with twice the lattice constant compared to the microscopic electron model. (This doubled unit cell is the minimal size needed to define the local AF and d -wave SC order parameters.) Therefore, each site x in the effective model corresponds to a plaquette of the microscopic electron model. (On a ladder, this corresponds to going from the lattice sites to ladder rungs.) The SO(5) singlet state $|\Omega\rangle$ corresponds to a resonating valence bond ‘‘(RVB)’’ type of singlet state, while the fivefold states $t_a^\dagger|\Omega\rangle$ describe the triplet magnon states, and the d -wave hole and particle pair states on a plaquette. Unlike the ladder case, the magnon and the d -wave pair states could condense in the ground state to form AF and SC broken symmetry states. In fact, Eder²⁵ has recently shown that properties of the AF states can be described by a coherent state of magnon condensation on top of a uniform spin liquid state. Our model therefore describes competition among the ‘‘RVB’’ type of singlet vacuum and the two forms of broken symmetry order.

While it is reasonable to take J and V to be approximately equal for magnons and pairs, the gap energy Δ for the neutral magnons and the charged pairs are very different in the insulating state at half-filling. In fact, their difference is of the order of the insulating gap U at half-filling. Taking into account the hard-core condition and neglecting the nearest-neighbor interaction V for now (it has higher powers of time and space derivatives in the continuum limit), we can express the general anisotropic SO(5) model as

$$H = \Delta_s \sum_x t_\alpha^\dagger t_\alpha(x) + \Delta_c \sum_x t_i^\dagger t_i(x) - J_s \sum_{\langle xx' \rangle} n_\alpha(x) n_\alpha(x') - J_c \sum_{\langle xx' \rangle} n_i(x) n_i(x'). \quad (2.6)$$

In this paper we shall use the convention where $a, b, \dots = 1, 2, 3, 4, 5$ denote the superspin indices, $\alpha, \beta, \dots = 2, 3, 4$ denote the spin indices, and $i, j = 1, 5$ denote the charge indices, and repeated indices are summed over. The main focus of our paper is to consider the limit where $\Delta_c \gg \Delta_s$.

Let us define the charge eigenoperators t_h and t_p as

$$t_1 = \frac{1}{\sqrt{2}}(t_h + t_p), \quad t_5 = \frac{1}{i\sqrt{2}}(t_h - t_p). \quad (2.7)$$

From this definition, it is clear that t_h^\dagger is the creation operator for a hole pair and t_p^\dagger is the creation operator for a particle pair. We can introduce a chemical potential term

$$H_\mu = \mu \sum_x [t_p^\dagger t_p(x) - t_h^\dagger t_h(x)] \quad (2.8)$$

to describe the effects of doping. In the presence of this chemical potential term, the gap energy of the hole and particle pairs are $\Delta_c - \mu$ and $\Delta_c + \mu$, respectively. A chemical potential of the order of the charge gap Δ_c is needed to induce a metal-insulator transition in this system. Near such a transition point, the gap energy of the hole pair

$$\tilde{\Delta}_c = \Delta_c - \mu \quad (2.9)$$

can be comparable to the spin gap Δ_s , while the gap towards a particle pair excitation is of the order of twice the charge gap, and needs to be projected out of the spectrum in the low-energy limit.

Therefore, within this formalism, the Gutzwiller projection is equivalent to restricting ourselves to the projected Hilbert space where

$$t_p(x)|\Psi\rangle = 0 \quad (2.10)$$

at every site x . Within this projected Hilbert space, the projected Hamiltonian takes the form

$$H = \Delta_s \sum_x t_\alpha^\dagger t_\alpha(x) + \tilde{\Delta}_c \sum_x n_i(x) n_i(x) - J_s \sum_{\langle xx' \rangle} n_\alpha(x) n_\alpha(x') - J_c \sum_{\langle xx' \rangle} n_i(x) n_i(x'). \quad (2.11)$$

This Hamiltonian has no parameters of the order of U , and it is reasonable to expect $\Delta_s \sim \tilde{\Delta}_c$ and $J_s \sim J_c$. We see that the form of the Hamiltonian hardly changes from the unprojected model, but the definition of n_1 and n_5 is changed from

$$n_1 = \frac{1}{\sqrt{2}}(t_1 + t_1^\dagger) = \frac{1}{2}(t_h + t_p + t_h^\dagger + t_p^\dagger),$$

$$n_5 = \frac{1}{\sqrt{2}}(t_5 + t_5^\dagger) = \frac{1}{2i}(t_h - t_p - t_h^\dagger + t_p^\dagger) \quad (2.12)$$

to

$$n_1 = \frac{1}{2}(t_h + t_h^\dagger), \quad n_5 = \frac{1}{2i}(t_h - t_h^\dagger). \quad (2.13)$$

From Eq. (2.12), we see that n_1 and n_5 commute with each other before the projection. However, after the projection, they acquire a nontrivial commutation relation, as can be seen from Eq. (2.13):

$$[n_1, n_5] = i/2. \quad (2.14)$$

Therefore, the Gutzwiller projection can be analytically implemented in the SO(5) theory by retaining the form of the Hamiltonian and change only the quantization condition.

III. ANALOGY WITH LOWEST-LANDAU-LEVEL PROJECTION

The discussions outlined above reveal a deep connection between the Gutzwiller projection within the SO(5) formalism and the projection onto the lowest Landau level (LLL) in the context of the fractional quantum Hall effect. Consider the problem of a charged particle in a strong magnetic field B and a rotationally symmetric potential $V(X, Y)$. In the absence of a magnetic field, all eigenstates form irreducible representations of the two-dimensional rotation group O(2), characterized by integral eigenvalues of the angular momentum operator

$$L_Z = XP_Y - YP_X. \quad (3.1)$$

However, in the presence of a strong magnetic field and projected into the LLL, only negative eigenvalues of L_Z are realized. This is analogous to the situation encountered here. The local charge operator in the SO(5) theory takes the form of the angular momentum in the n_1 - n_5 plane as given by Eq. (1.1). When doubly occupied sites are locally projected out, the local charge operator, or the angular momentum in the n_1 - n_5 plane, takes only negative values. Since the chemical potential couples directly the angular momentum in the n_1 - n_5 plane, it plays the role of a fictitious magnetic field threading every SO(5) rotor in the n_1 - n_5 plane. The Landau level spacing $\hbar\omega_c$ is analogous to the charge gap Δ_c encountered here, and both are taken to be infinity in the projected models. After the projection, the Hamiltonian in the Landau level problem retains its O(2) symmetric form,

$$H = V(X, Y) \quad (3.2)$$

although a new quantization condition is imposed between X and Y , as given by Eq. (1.3). This is analogous to the observation we made here that the Hamiltonian formally retains a SO(5) symmetric form after the projection (2.10), but the quantum dynamics is changed due to the nontrivial commutator between n_1 and n_5 . In both cases only a part of the full symmetry multiplets remain after the projection. However, the formal symmetry of the Hamiltonian has direct physical manifestations despite the projection. For example, in the LLL problems, semiclassical orbits of the guiding center coordinates are still O(2) symmetric. In our case, we shall see that the static potential for the superspin vector can still be SO(5) invariant despite the projection.

Perhaps the most explicit way to establish the precise connections between these two problems is to consider the constraints on the wave function. In the symmetric gauge of the LLL problem, the annihilation operator for the cyclotron coordinates takes the form²⁴

$$a = \partial_{\bar{z}} + z/4, \quad (3.3)$$

where $z = X + iY$ and $\bar{z} = X - iY$. Projection onto LLL requires

$$a\Psi(z, \bar{z}) = 0, \quad (3.4)$$

which determines the form of the LLL wave function to be

$$\Psi(z, \bar{z}) = f(z) e^{-z\bar{z}/4}, \quad (3.5)$$

where $f(z)$ is a holomorphic function of z only. This holomorphic condition also places strong constraints in many-body systems and led to the celebrated Laughlin's wave function. Our no-double-occupancy constraint (2.10) is analogous to the LLL constraint (3.4). In fact from Eqs. (2.7) and (2.12), we obtain

$$t_p = \frac{1}{2}(z + 2\partial_{\bar{z}}), \quad (3.6)$$

where $z = n_1 - in_5$ and $\bar{z} = n_1 + in_5$. For a single unprojected SO(5) rotor, the wave function $\Psi(n_a)$ is a function of the superspin coordinates. However, the Gutzwiller projection (2.10) restricts the wave function to be

$$\Psi(n_1, n_2, n_3, n_4, n_5) = f(z = n_1 - in_5, n_2, n_3, n_4) e^{-z\bar{z}/2}, \quad (3.7)$$

where $f(z, n_2, n_3, n_4)$ is a holomorphic function of z . For a collection of SO(5) rotors, the superspin coordinates are themselves functions of the lattice sites x , and $\Psi[n_a(x)]$ is a functional of the superspin coordinates at each site. For the projected SO(5) models, this functional is restricted to take the form

$$\Psi[n_a(x)] = f(z(x), n_a(x)) \prod_x e^{-z\bar{z}(x)/2}, \quad (3.8)$$

where $f(z(x), n_a(x))$ is a holomorphic functional of $z(x) = n_1(x) - in_5(x)$.

The formal but precise analogy between the two types of projection allows us to introduce the concept of a chiral SO(5) rotor. This is a system of rotors with SO(5) invariant potential and coupling, however, the rotation within the n_1 - n_5 plane is chiral, i.e., only one sense of the rotation is allowed. Such a system of chiral SO(5) rotors is described by the wave functional in Eq. (3.8).

IV. SO(5) SYMMETRY OF THE GROUND-STATE ENERGY

Having discussed the general notions of the projected SO(5) model, we are now in a position to explore the phase diagram of this model. As we commented earlier, the projected SO(5) model describes the competition and unification of the spin liquid, AF and the SC states. In the original unprojected SO(5) symmetric model, not only are the AF and SC states degenerate in energy, but they are also degenerate with all the intermediate coexistence states. This points out a route from AF to SC with no potential barrier, and introduces the concept that the metal-insulator transition in the high- T_c systems can be viewed as a smooth rotation of the SO(5) superspin. One of the key questions to be answered in this work is what happens to the picture in the case of projected SO(5) symmetry.

In anticipation of the competition of the states discussed above, we construct a class of variational wave functions in the coherent state representation:

$$|\Psi\rangle = \prod_x \{ \cos \theta(x) + \sin \theta(x) [m_\alpha(x) t_\alpha^\dagger(x) + \Delta(x) t_h^\dagger(x)] \} |\Omega\rangle. \quad (4.1)$$

Here $|\Omega(x)\rangle$ denotes a local singlet state defined by $t_\alpha(x)|\Omega(x)\rangle = t_h(x)|\Omega(x)\rangle = 0$ and $|\Omega\rangle$ is a product state of these local singlets, $|\Omega\rangle = \prod_x |\Omega(x)\rangle$. $\theta(x)$ is a local variational parameter describing the competition between long-range order and quantum disorder. For $\theta(x) = 0$ our variational wave function describe a spin singlet ground state, while a nonzero value of θ describes a coherent state formed by the local singlet, the magnon, or the hole pair state. This wave function is a generalization of the coherent state description of a AF state in terms of a magnon condensate.^{6,25} As we shall see from Eq. (4.2), $\sin 2\theta$ stands for the length of the SO(5) superspin vector. $m_\alpha(x)$ and $\Delta(x)$ are general complex variational parameters describing the local amplitude for magnons and hole pairs. We notice that this wave function satisfies both the Gutzwiller constraint (2.10) and the hard-core constraint for magnons and hole pairs exactly. It is easy to see that

$$\begin{aligned}\langle\Psi|n_\alpha(x)|\Psi\rangle &= \frac{1}{\sqrt{2}}\sin 2\theta(x)\text{Re}[m_\alpha(x)], \\ \langle\Psi|n_1(x)|\Psi\rangle &= \frac{1}{2}\sin 2\theta(x)\text{Re}[\Delta(x)], \\ \langle\Psi|n_5(x)|\Psi\rangle &= \frac{1}{2}\sin 2\theta(x)\text{Im}[\Delta(x)],\end{aligned}\quad (4.2)$$

where Re and Im denote the real and imaginary parts of a complex number. The coupling terms in the projected SO(5) Hamiltonian depend only on $n_\alpha(x)$, $n_1(x)$, and $n_5(x)$. Therefore, the coupling energy depends only on the real part of $m_\alpha(x)$ while it depends on both the real and imaginary parts of $\Delta(x)$. Therefore, for discussing the ground-state wave functions, we can assume without loss of generality that $m_\alpha(x)$ is real and $\Delta(x) = m_1(x) + im_5(x)$. The normalization condition $\langle\Psi|\Psi\rangle = 1$ can be implemented by the constraint that

$$m_\alpha^2(x) = (m_1^2 + m_5^2 + m_\alpha^2)(x) = 1. \quad (4.3)$$

Therefore, we see that although we have completely projected out the particle pair states, the local degrees of freedom can still be represented by a vector on a five-dimensional sphere.

Uniform states are obtained by taking all parameters to be constant. For $\Delta = 0$ and $\sin 2\theta \neq 0$, our wave function $|\Psi\rangle$ describes a pure AF state with the following properties:

$$\begin{aligned}\langle\Psi|Q|\Psi\rangle &= \langle\Psi|\sum_x t_h^\dagger t_h(x)|\Psi\rangle = 0, \\ \langle\Psi|N_\alpha|\Psi\rangle &= \langle\Psi|\sum_x n_\alpha(x)|\Psi\rangle = N\frac{1}{\sqrt{2}}\sin 2\theta m_\alpha, \\ \langle\Psi|S_\alpha|\Psi\rangle &= \langle\Psi|\sum_x i\epsilon^{\alpha\beta\gamma}t_\beta^\dagger t_\gamma(x)|\Psi\rangle = 0,\end{aligned}$$

$$\begin{aligned}\langle\Psi|S^2|\Psi\rangle &= \langle\Psi|\left(\sum_x S(x)\right)^2|\Psi\rangle \\ &= N2\sin^2\theta + N\sin^4\theta(1 - m_\alpha^4),\end{aligned}\quad (4.4)$$

where N is the number of lattice sites. Equation (4.4) describes a half-filled state with a macroscopic Néel magnetization, and vanishing uniform magnetization. Furthermore, this state is composed as a linear superposition of eigenstates with different values of the total spin, and the fluctuation of the total spin scales like $\sqrt{\langle S^2\rangle} \propto \sqrt{N}$, just as one expects from a standard Néel state.

On the other hand, for $m_\alpha = 0$ and $\sin 2\theta \neq 0$, $|\Psi\rangle$ describes a pure SC state with the following properties:

$$\begin{aligned}\langle\Psi|Q|\Psi\rangle &= \langle\Psi|\sum_x t_h^\dagger t_h(x)|\Psi\rangle = N\sin^2\theta, \\ \langle\Psi|N_1 + iN_5|\Psi\rangle &= \langle\Psi|\sum_x (n_1 + in_5)(x)|\Psi\rangle \\ &= N\frac{1}{2}\sin 2\theta(m_1 + im_5), \\ \langle\Psi|Q^2|\Psi\rangle - \langle\Psi|Q|\Psi\rangle^2 &= N\sin^2\theta\cos^2\theta.\end{aligned}\quad (4.5)$$

Equation (4.5) describes a state with a finite doping density and a finite SC order parameter. Just as in the standard BCS case, this state is composed as a linear superposition of eigenstates with different values of the total charge, and the fluctuation of the total charge scales like $\sqrt{\langle Q^2\rangle - \langle Q\rangle^2} \propto \sqrt{N}$, just as one expects from a standard SC state.

However, besides these two *pure* states, there is a class of *mixed* states which interpolates between the pure AF and SC states. Taking $m_1 = \sin\alpha$ and $m_2 = \cos\alpha$, we see that the mixed states have the following property:

$$\begin{aligned}\langle\Psi|Q|\Psi\rangle &= N\sin^2\theta\sin^2\alpha, \\ \langle\Psi|N_1 + iN_5|\Psi\rangle &= N\frac{1}{2}\sin 2\theta\sin\alpha, \\ \langle\Psi|N_2|\Psi\rangle &= N\frac{1}{\sqrt{2}}\sin 2\theta\cos\alpha.\end{aligned}\quad (4.6)$$

Therefore, we see that there is a continuous family of intermediate mixed states interpolating between the pure AF state at half-filling and the pure SC state with finite doping density. As the SO(5) angle α rotates continuously from a pure AF state with $\alpha = 0$ to a pure SC state with $\alpha = \pi/2$, the hole density of the mixed state interpolates continuously between these two limits. Therefore, our wave function gives a unified description of AF and SC and points out a precise route from AF to SC as the doping level is varied. In order for this route, or small deviations from this route, to be physically realized in the high- T_c superconductors, we have to demonstrate that there is no large energy barrier for the intermediate mixed states, or that the ground-state energy is approximately independent of the SO(5) mixing angle α . In particular, we have to show that the energy barrier is independent of

the Hubbard energy U , in the limit of large U . In the following, we shall investigate this question.

The energy functional $\langle \Psi | H | \Psi \rangle$ describes the coupling between these five-dimensional vectors $m_a(x)$, and it is given by

$$\begin{aligned} \langle \Psi | H | \Psi \rangle &= E(\theta(x), m_a(x)) \\ &= -\frac{J_s}{2} \sum_{xx'} \sin 2\theta(x) \sin 2\theta(x') m_a(x) m_a(x') \\ &\quad - \frac{J_c}{4} \sum_{xx'} \sin 2\theta(x) \sin 2\theta(x') m_i(x) m_i(x') \\ &\quad + \Delta_s \sum_x \sin^2 \theta(x) m_\alpha^2(x) \\ &\quad + \tilde{\Delta}_c \sum_x \sin^2 \theta(x) m_i^2(x). \end{aligned} \quad (4.7)$$

This ground-state energy functional describes a systems of coupled rotors satisfying the constraint (4.3). At the point $J_c = 2J_s$ and $\tilde{\Delta}_c = \Delta_s$ in parameter space, this rotor model is exactly SO(5) symmetric. This is a central observation of this work.

From this consideration we learn a very important lesson about the compatibility of the Mott insulating gap and the idea of a smooth SO(5) rotation from AF to SC. As we have seen, the large asymmetry between the charge and spin gap at half-filling necessitates the removal of the $Q(x) > 0$ part of the SO(5) multiplets; therefore, the dynamics close to half-filling has to be modified. But the static potential governing the transition from AF to SC can remain SO(5) symmetric, and in particular, the energy barrier separating these two states can remain small in the limit where the Mott insulating gap tends to infinity.

We also observe a crucial difference between the projected and the unprojected SO(5) models. In the unprojected SO(5) model with the full SO(5) symmetry, AF and SC states are degenerate at half-filling, and the rotation between these two states can be continuously performed without changing the density to going away from half-filling. This case is similar to the well-known degeneracy between the charge-density wave state and the s -wave SC state for the negative U Hubbard model at half-filling. In the projected SO(5) model, where all particle pair states have been locally removed, the SO(5) rotation from the AF to SC states are accompanied by the continuous change of the hole density, and a pure SC state can only be reached at a finite critical hole doping density $\rho_c = \sin^2 \theta$. While the unprojected SO(5) symmetry is only valid at half-filling, the projected SO(5) symmetry can be valid for a range of doping concentration $0 < \rho < \rho_c$, since all these doping concentrations correspond to the same value of the chemical potential $\mu = \mu_c$ at which the ground-state energy (4.7) is SO(5) symmetric.

However, it should be pointed out that the projected SO(5) symmetry at $\mu = \mu_c$ has only been demonstrated within the variational mean-field approximation. This corresponds to the semiclassical limit, and becomes exact only in the large s limit, where s labels the representation of the local SO(5) group at a given site. Quantum fluctuations can be

systematically investigated as a $1/s$ expansion. Assuming uniform ground states, we have studied the effect of zero point fluctuations in Sec. VII and found that at $\mu = \mu_c$, the intermediate mixed states have slightly higher energy than the AF and SC state. Therefore, quantum fluctuation leads to a slight breaking of the projected SO(5) symmetry. The important point here is that this symmetry breaking effect can be systematically controlled in the semiclassical $1/s$ expansion, and certainly is independent of the Coulomb energy scale U . This fluctuation would induce a first-order transition and predict phase separation of AF and SC states at $\mu = \mu_c$. However, there are also other competing interactions such as nearest-neighbor and next-nearest-neighbor interactions which tend to reduce the barrier, and could also lead to nonuniform states like stripes. Due to the complexity of the calculations, we shall defer the detailed studies of these competing effects to future works.

V. PHASE DIAGRAM

In this section we investigate the phase diagram of the projected SO(5) model within the framework of the variational wave function (4.1). Taking uniform values of the variational parameters θ , $m_x = \cos \alpha$, $m_1 = \sin \alpha$, and $m_y = m_z = m_5 = 0$, the variational energy in Eq. (4.7) reduces to

$$\begin{aligned} \frac{E(\theta, \alpha)}{N} &= -J_s \sin^2 2\theta \cos^2 \alpha - \frac{J_c}{2} \sin^2 2\theta \sin^2 \alpha \\ &\quad + \Delta_s \sin^2 \theta \cos^2 \alpha + \tilde{\Delta}_c \sin^2 \theta \sin^2 \alpha. \end{aligned} \quad (5.1)$$

In the following, we shall mainly study the SO(5) symmetric case, and take $J_c = 2J_s = 2J$. Defining $x = \sin^2 \theta$ and $y = \cos^2 \alpha$, and the dimensionless coupling constants $\epsilon \equiv E(x, y)/4JN$, $\delta_s \equiv \Delta_s/4J$ and $\tilde{\delta}_c \equiv \tilde{\Delta}_c/4J$, we obtain

$$\epsilon(x, y) = x^2 - x + \tilde{\delta}_c x + (\delta_s - \tilde{\delta}_c) xy. \quad (5.2)$$

We shall minimize Eq. (5.2) with respect to x and y , subject to the condition that $0 \leq x, y \leq 1$. The phase diagram can be plotted in the two-dimensional parameter space of $\tilde{\delta}_c$ and δ_s . We notice that $\epsilon(x, y)$ depends linearly on y : therefore, for $\delta_s > \tilde{\delta}_c$ we obtain $y_{min} = 0$ and

$$\begin{aligned} 0 < x_{min} &= \frac{1 - \tilde{\delta}_c}{2} < 1 \quad \text{for} \quad -1 < \tilde{\delta}_c < 1, \\ x_{min} &= 0 \quad \text{for} \quad \tilde{\delta}_c > 1, \\ x_{min} &= 1 \quad \text{for} \quad \tilde{\delta}_c < -1. \end{aligned} \quad (5.3)$$

Similarly, for $\delta_s < \tilde{\delta}_c$ we obtain $y_{min} = 1$ and

$$\begin{aligned} 0 < x_{min} &= \frac{1 - \delta_s}{2} < 1 \quad \text{for} \quad -1 < \delta_s < 1, \\ x_{min} &= 0 \quad \text{for} \quad \delta_s > 1, \\ x_{min} &= 1 \quad \text{for} \quad \delta_s < -1. \end{aligned} \quad (5.4)$$

From these equation, we can determine the phase diagram as shown in Fig. 2.

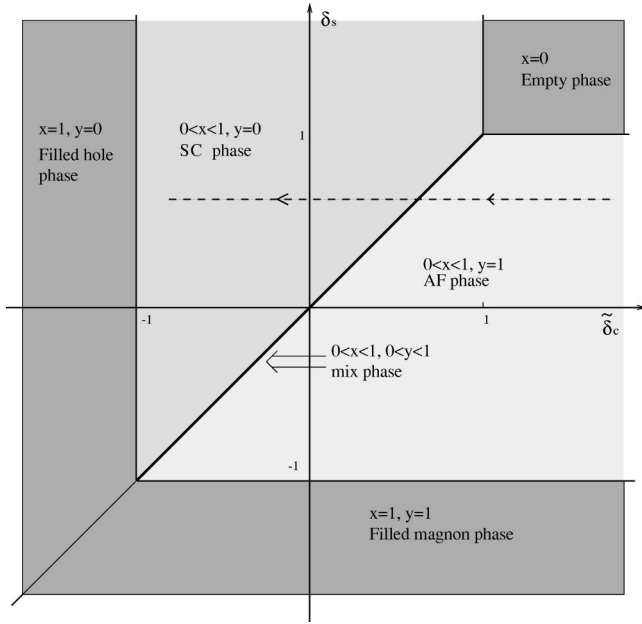


FIG. 2. Phase diagram of the projected SO(5) model in the δ_s versus $\tilde{\delta}_c$ plane. Phase boundaries are depicted by the solid lines. Variation of the chemical potential traces out a one-dimensional trajectory as shown on the dotted line.

There are seven different phases on this phase diagram. $x_{min}=0$ corresponds to a quantum disordered singlet state with no condensed bosons. $x_{min}=1$ and $y_{min}=0$ correspond to a quantum disordered state with completely filled hole pairs. $x_{min}=1$ and $y_{min}=1$ correspond to a quantum disordered state with completely filled magnons. $0 < x_{min} < 1$ and $y_{min}=1$ describe a pure AF phase, while $0 < x_{min} < 1$ and $y_{min}=0$ describe a pure SC phase. When $-1 < \delta_s < \tilde{\delta}_c < 1$ a continuous family of mixed AF/SC states labeled by a free superspin angle $0 < \alpha < \pi/2$ is realized, while for $\delta_s = \tilde{\delta}_c < -1$ a continuous family of quantum disordered states labeled by a free superspin angle $0 < \alpha < \pi/2$ is obtained.

The system traces out a one-dimensional trajectory in this two-dimensional phase diagram as the chemical potential is increased, as depicted in Fig. 2. Increasing the chemical potential decreases the $\tilde{\delta}_c$ parameter while holding δ_s constant. δ_s describes the degree of quantum spin fluctuations in the system, since in the AF phase, the size of the Néel moment

$$m_{AF} = \sqrt{\frac{1}{2}(1 - \delta_s^2)} \quad (5.5)$$

decreases with increasing δ_s . For $\delta_s < 1$, the system goes through a phase transition from AF to SC at $\mu = \mu_c = \Delta_c - \Delta_s$. At this critical value of the chemical potential, the θ parameter remains fixed, but the α parameter changes continuously from 0 to $\pi/2$, and correspondingly, the density changes from 0 to

$$\rho_c \equiv \sin^2 \theta = x_{min} = \frac{1 - \delta_s}{2}. \quad (5.6)$$

This behavior gives a density versus chemical potential diagram as shown in Fig. 3.

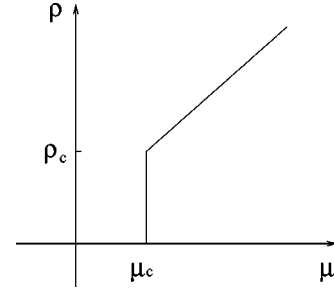


FIG. 3. Density versus chemical potential relation in the projected SO(5) model. Unlike the case of a generic first-order transition, the ground state in the density range $0 < \rho < \rho_c$ is uniform, rather than phase separated.

As we see, for densities in the range $0 < \rho < \rho_c$, the system is infinitely compressible since $\partial\rho/\partial\mu = \infty$. For $\mu > \mu_c$ or $\rho > \rho_c$, the system has a finite compressibility of $\partial\rho/\partial\mu = 1/8J$.

It is interesting to plot both the AF and the SC order parameters $\langle n_1 \rangle$ and $\langle n_2 \rangle$ as a function of the density for the whole range of $0 < \rho < 1$. We will restrict ourselves to the case of $0 < \delta_s < 1$ where the undoped state is an AF state. We obtain the following doping dependence of the SC order parameter:

$$\langle n_1 \rangle = \begin{cases} \sqrt{\rho(1 - \rho_c)} & \text{for } \rho < \rho_c, \\ \sqrt{\rho(1 - \rho)} & \text{for } \rho > \rho_c. \end{cases} \quad (5.7)$$

and the doping dependence of the AF order parameter:

$$\langle n_2 \rangle = \begin{cases} \sqrt{2(1 - \rho_c)(\rho_c - \rho)} & \text{for } \rho < \rho_c, \\ 0 & \text{for } \rho > \rho_c. \end{cases} \quad (5.8)$$

These behaviors are depicted in Fig. 4.

We note several interesting features of the phase diagram. First of all, we can use the energy functional (4.7) as a starting point for a finite-temperature classical fluctuation analysis, and estimate the transition temperature due to the classical fluctuations. Within such a framework, the three-dimensional AF (T_N) and SC (T_c) transition temperatures are proportional to the stiffness of the spin and the phase fluctuations, which are in turn proportional to $\langle n_2 \rangle^2$ and $\langle n_1 \rangle^2$, respectively. Therefore, Fig. 4 gives an approximate estimate of the transition temperatures. For small ρ_c , we see that there is a sharp drop of T_N and a maximum of T_c at $\rho = 1/2$. The system is an AF insulator at doping $\rho = 0$ and a pure SC state for $\rho > \rho_c$. The reason for a maximum of T_c at $\rho = 1/2$ is due to the strong correlation of the charged bosons. The charge bosons have a hard-core interaction, therefore, they are insulating at both $\rho = 0$ and $\rho = 1$ and have maximal

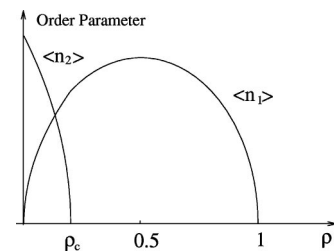


FIG. 4. AF ($\langle n_2 \rangle$) and SC ($\langle n_1 \rangle$) order parameters versus density in the projected SO(5) model.

charge stiffness at $\rho=1/2$. We can perform a rough translation of this optimal doping value in our effective model to the microscopic model. Since our effective model is defined on a unit cell with twice the lattice spacing of the microscopic model, $\rho=1/2$ therefore describes one hole pair per four sites in the microscopic model, or a doping of $x=1/4=25\%$ in the conventional language. This crude argument tends to overestimate the value for optimal doping, since it neglects the effects of unpaired electrons. However, considering the crudeness of the estimate, it is still reasonably close to the optimal doping $x=15\%$ observed in the La-Sr-Cu-O family of high- T_c superconductors.

In the regime of $0<\rho<\rho_c$, the system is a coherent mixture of AF and SC order. For this entire range of densities, the system has a projected SO(5) symmetry within the variational approximation discussed above. The projected SO(5) symmetry manifests itself in terms of a infinite compressibility in the region $0<\rho<\rho_c$ and, as we shall see in next section, a charge mode with a dispersion relation $\omega\sim k^2$. Since such a state is rather unusual, and maybe highly susceptible to density fluctuations, we would like to discuss more detailed physical properties in this region.

First let us comment on the fact that there are familiar physical systems whose uniform ground states are infinitely compressible. The free boson model is certainly such an example, and the density mode also has a $\omega\sim k^2$ dispersion relation. But the infinite compressibility is due to the absence of the interaction, which is not characteristic of the strongly interaction system considered here. A less trivial example is the spin-1/2 XXZ ferromagnetic Heisenberg model, given by the Hamiltonian,

$$\mathcal{H}=J\sum_{i,j}(S_i^xS_j^x+S_i^yS_j^y+\Delta S_i^zS_j^z), \quad (5.9)$$

where $J<0$ and the sum extends over nearest-neighbor sites of a square lattice. This model can be interpreted as quantum hard-core boson model, where the fully polarized spin-down state could be identified with the vacuum of the bosons, the XY part of the Hamiltonian describes the hopping of the bosons, and the last term describes the nearest-neighbor attraction between the bosons if $\Delta>0$. When $\Delta>1$, the system is in the Ising limit, and the spontaneous breaking of the Z_2 symmetry implies phase separation of the bosons. On the other hand, when $0<\Delta<1$, the system is in the XY limit, and the ground state is a superfluid. Therefore, the anisotropy parameter describe the competition between superfluidity and phase separation. At $\Delta=1$, the system has a SU(2) symmetry and the dispersion relation becomes quadratic. Different directions of the ferromagnetic polarizations are degenerate and can be changed without any energy cost. Since the z component of the ferromagnetic polarization is identified with the total density of the hard-core bosons, the SU(2) vacuum degeneracy implies infinite compressibility of the corresponding boson system for the entire range of boson densities $0<\rho<1$.

These two examples illustrate that there is nothing intrinsically pathological about having a system with infinite compressibility. The second example is more generic, and shows that uniform states with infinite compressibility can be obtained in systems on the verge of phase separation, and the

infinite compressibility can be ensured by symmetry. Both of these properties are also shared by the projected SO(5) model. These models are on the verge of phase separation into AF and SC phases, and the infinite compressibility is a result of the projected SO(5) symmetry. It indicates that small perturbations, such as next-nearest-neighbor interactions, quantum fluctuations, and quenched disorder, will be very important to determine the true ground state. With such perturbations, the ground state is expected to be unstable toward the experimentally reported textures such as the spin glass, stripes, and incommensurate spin-density waves.

Next let us investigate the phenomenological consequence of this remarkable property. One of the most puzzling properties of the high- T_c superconductors is the constant chemical potential in the underdoped samples. For La-Sr-Cu-O systems, where the doping level can be varied continuously by the Sr concentration, this effect has been dramatically observed in the angle-resolved photoemission spectroscopy (ARPES) experiments and the constant chemical potential persists from the weakly doped insulator to the optimally doped superconductor.²⁶ In fact numerical calculations on the Hubbard model also reveal similar divergent behavior of the compressibility as the metal-insulator transition is approached from the metallic side.²⁷

The simplest explanation of the small chemical potential shift is a two-phase mixture with different densities at a first-order phase transition. If the system globally phase separates into two different spatial regions with different charge densities but the same free energy densities, the added charges only change the proportion of mixture of the two phases and do not change the energy, therefore, $\partial\mu/\partial\rho=0$. However, this situation of global phase separation can certainly not occur in a system with long-ranged Coulomb interaction and is ruled out in the real high- T_c system.

A phenomenon possibly related to the tendency of phase separation is the formation of stripes.²⁸⁻³⁰ A stripe state can be viewed as microscopic phase separation of AF and SC into alternating regions, where each region has different charge density and the same free energy density. However, a crucial difference between the global phase separation and this picture of microscopic phase separation is that the stripe state has infinitely many surfaces between AF and SC, and the surface energy makes a finite contribution to the total energy in the thermodynamic limit. In this picture, doping can be accomplished by converting AF stripes into SC stripes, thereby creating more surfaces separating AF and SC regions. Finite doping density therefore leads to a finite density of surfaces and the accumulated surface energy would in general lead to a shift of the chemical potential *under a generic situation*. Additional physical conditions are needed to ensure the constant chemical potential in the stripe phase.

Therefore, the absence of the chemical potential shift places a very strong constraint on possible theoretical explanations. The projected SO(5) model proposed in this work offers a possible explanation for the absence of chemical potential shift. At a critical value of the chemical potential where the AF and SC states have degenerate energy density, we can have three situations, where the intermediate mixed states have higher, lower, or degenerate energy compared to the AF and SC states. When the intermediate states have higher energy, the system will go through a first-order phase

transition at $\mu = \mu_c$ and this will lead to global phase separation into AF and SC regions. On the other hand, if the intermediate states have lower energy, there exists a range of chemical potential $\mu_{c1} < \mu < \mu_{c2}$ where the mixed phase has a uniform and continuously varying density. In this case, $\partial\mu/\partial\rho \neq 0$ is obtained. When the region $\mu_{c1} < \mu < \mu_{c2}$ shrinks to zero, we obtain the limiting SO(5) symmetric case where the system is on the boundary between a first-order transition and two second-order phase transitions. In this case, $\partial\mu/\partial\rho = 0$ for a range of densities $0 < \rho < \rho_c$. Therefore, if we restrict ourselves to ground states where the density is not globally inhomogeneous, the absence of the chemical shift directly implies SO(5) symmetry.

Within this model, we can therefore define a experimental procedure to measure one of the most crucial parameters of the theory, namely ρ_c . Using the experimental ARPES data for La-Sr-Cu-O system we would identify ρ_c to be approximately the same as the optimal doping density. We recall that ρ_c is also a measure of the degree of the quantum spin fluctuation in the system. For the bilayer materials such as Y-Ba-Cu-O and Bi-Sr-Ca-Cu-O superconductors, the quantum spin fluctuation are stronger due to the interlayer spin exchange, and we would predict that ρ_c should be less than the optimal doping value.

VI. COLLECTIVE MODES

Having discussed the ground-state properties and the phase diagram of the model, we are now in a position to study the collective excitations of the model. We have argued that the ground-state energy can remain SO(5) symmetric despite the projection. However, the projection does affect the collective excitation spectrum near half-filling. Nonetheless, as we shall see, there remains a unique signature of the projected SO(5) symmetry in the collective excitation spectra.

In principle, the collective excitation spectra can be obtained straightforwardly by studying the quadratic fluctuations around the mean-field minima. The resulting quadratic boson Hamiltonian can be simply diagonalized. The main complication in the procedure is the hard-core boson constraint, which requires

$$t_a^\dagger t_a(x) + t_h^\dagger t_h(x) \leq 1 \quad (6.1)$$

for every site. There are several ways to implement this constraint rigorously. One is to follow the mapping from the one-component hard-core boson model to the XY model and generalize it to a multicomponent hard-core boson model. One could also convert the above inequality constraint to an equality constraint by introducing a boson creation and annihilation operator for the singlet state. This approach will be implemented in the Appendix. For simplicity of presentation, here we shall adopt a less rigorous approach and introduce an on-site boson repulsion term

$$W \sum_x (t_a^\dagger t_a + t_h^\dagger t_h)^2 \quad (6.2)$$

to our Hamiltonian (2.11) and convert the hard-core constraint to a soft-core constraint. We shall show later that all results can be expressed in terms of the order parameter,

which is implicitly dependent on W , but there is no explicit dependence on W . We have verified that all three methods give the same long-wavelength spectra for the collective modes in the limit of low boson density. In the next section, we shall present another calculation based on the continuum effective Lagrangian method, which also reproduces the same spectra.

To simplify presentation, we shall concentrate on the case where the ground-state energy functional (4.7) is SO(5) symmetric, i.e., for coupling constants $J_c = 2J_s = 2J$ and $\tilde{\Delta}_c = \Delta_s = \Delta$. We choose the direction of spontaneously broken symmetry to be $\langle t_x \rangle = \langle t_x^\dagger \rangle = x$ and $\langle t_h \rangle = \langle t_h^\dagger \rangle = y$. The extremal condition can be easily determined to be

$$x^2 + y^2 \equiv r^2 = \frac{4J - \Delta}{2W}. \quad (6.3)$$

The combination $x^2 + y^2$ expresses the fact that the classical minimum is SO(5) symmetric. We can therefore write $x = r \cos \alpha$ and $y = r \sin \alpha$. Expanding the boson operators as

$$t_x = x + a_x, \quad t_y = a_y, \quad t_z = a_z, \quad t_h = y + a_h, \quad (6.4)$$

we obtain the following quadratic Hamiltonian

$$\begin{aligned} H = & (\Delta + 2Wr^2) \sum_x (a_x^\dagger a_x + a_h^\dagger a_h) + Wx^2 \sum_x (a_x^\dagger + a_x)^2 \\ & + Wy^2 \sum_x (a_h^\dagger + a_h)^2 - \frac{J}{2} \sum_{\langle x, x' \rangle} [a_x^\dagger(x) + a_x(x)] \\ & \times [a_x^\dagger(x') + a_x(x')] - J \sum_{\langle x, x' \rangle} [a_h^\dagger(x) a_h(x') + \text{H.c.}] \\ & + 2Wxy \sum_x [a_h^\dagger(x) + a_h(x)] [a_x^\dagger(x) + a_x(x)] \\ & - \frac{J}{2} \sum_{\langle x, x' \rangle} [a_y^\dagger(x) + a_y(x)] [a_y^\dagger(x') + a_y(x')] \\ & - \frac{J}{2} \sum_{\langle x, x' \rangle} [a_z^\dagger(x) + a_z(x)] [a_z^\dagger(x') + a_z(x')] \\ & + (\Delta + 2Wr^2) \sum_x (a_y^\dagger a_y + a_z^\dagger a_z). \end{aligned} \quad (6.5)$$

We are in particular interested in the collective mode spectra for the AF insulating state with $\alpha = 0$, the mixed states with $0 < \alpha < \pi/2$, and the SC state with $\alpha = \pi/2$ and how they connect to each other.

From this quadratic Hamiltonian we can learn a number of important features. First we notice that the a_y and a_z modes are decoupled for all ranges of $0 \leq \alpha \leq \pi/2$, but most importantly, their dispersion relations are independent of α and given by

$$\omega(k) = v_s k, \quad v_s = 2J, \quad (6.6)$$

where $k \equiv a|\vec{k}|$ and a is the lattice constant. This is indeed a very remarkable property. At $\alpha = 0$, a_y and a_z modes are nothing but the transverse AF spin wave modes. AF spin waves are usually viewed as Goldstone modes and their ex-

istence is due to the AF long-range order. However, as α changes continuously from 0 to $\pi/2$, the AF long-range order continuously diminishes until it vanishes at $\alpha = \pi/2$. The reason that the properties of the a_y and a_z modes do not change at all is due to the SO(5) symmetry of this model, since the diminishing AF order is compensated by the increasing SC order as the superspin angle α is varied. As we shall see, the a_x mode is the AF spin amplitude mode at $\alpha = 0$, but it becomes massless and degenerate with the a_y and a_z modes at $\alpha = \pi/2$. These three modes form a massless π triplet mode whose existence is purely a consequence of the SC order. Therefore, as α is continuously varied from 0 to $\pi/2$, the transverse AF spin-wave modes gradually change their character to become the π triplet resonance of the SC state. As we shall see, for $\mu > \mu_c$, the π triplet mode becomes massive.

At the AF point $\alpha = 0$, the spin amplitude mode a_x is decoupled from the SC mode a_h and can be diagonalized separately. The dispersion for the spin amplitude mode has the conventional massive relativistic form for small k

$$\omega^2(k) = 16J^2(k^2/4 + m_x^2), \quad m_x^2 = \frac{Wx^2}{J} = \frac{4J - \Delta}{2J}. \quad (6.7)$$

On the other hand, we have a massless SC Goldstone mode a_h with the following dispersion:

$$\omega(k) = Jk^2. \quad (6.8)$$

This mode is an important prediction of the SO(5) theory. It is the counterpart of the π resonance in the AF state. In the unprojected SO(5) model, there are two such modes, with charge ± 2 , and they represent gapless fluctuations from AF to SC at half-filling. In the projected SO(5) model, the charge +2 mode is projected out of the spectrum, however, the charge -2 mode remain massless at $\mu = \mu_c$. It is also a manifestation of the gapless fluctuation from AF to SC at half-filling, but the SC fluctuation is holelike, rather than both holelike and particlelike as in the unprojected case. We see again that a large Mott-Hubbard gap is fully compatible with gapless SC fluctuation at half-filling. Experimental detection of this mode could provide a important test of the projected SO(5) symmetry.

The a_x and the a_h modes also decouple in the pure SC state with $\alpha = \pi/2$. However, their physical interpretation changes. The a_x mode becomes gapless at this point with the same dispersion as in Eq. (6.6). Therefore, the three modes a_x , a_y , and a_z form a gapless π triplet mode of the pure SC state, and represent the gapless fluctuation from SC to AF at $\mu = \mu_c$, but with a finite hole density ρ_c given in Eq. (5.6). The dispersion for the a_h mode is given by

$$\omega(k) = 2Jm_h k, \quad m_h^2 = \frac{Wy^2}{J} = \frac{4J - \Delta}{2J} \quad (6.9)$$

and has the natural interpretation of a linearly dispersing phase Goldstone mode of the SC state.

In the intermediate mixed state with $0 < \alpha < \pi/2$, the a_x and the a_h modes are coupled. Diagonalization of these modes gives

$$\frac{\omega^2(k)}{(4J)^2} = \begin{cases} (1 + m_h^2)k^2/4 + m_x^2, \\ (1 + m_h^2/m_x^2)k^4/16, \end{cases} \quad \begin{cases} m_x^2 = \frac{4J - \Delta}{2J} \cos^2 \alpha, \\ m_h^2 = \frac{4J - \Delta}{2J} \sin^2 \alpha. \end{cases} \quad (6.10)$$

The upper massive mode has predominantly spin amplitude character, and we see that the gap diminishes continuously until it reaches zero at $\alpha = \pi/2$ to become the massless π triplet mode. The lower mode has predominantly SC fluctuation character, and has a gapless $\omega \propto k^2$ dispersion. In the mixed region where both the AF and the SC order parameters are nonzero, one would naturally expect a gapless phase mode corresponding to the SC order. However, in a interacting boson system, the phase mode is expected to have linear dispersion on general ground. Therefore, what is interesting here is not the gapless nature of the SC mode, but its *quadratic dispersion*. In order to locate the origin of the quadratic dispersion, we have perturbed the model away from the projected SO(5) symmetric point so that a uniform mixed state is stabilized as a classical minimum. SC fluctuation around such a non-SO(5) symmetric point is gapless and has linear dispersion. A quadratic dispersion is only realized at the SO(5) symmetric point. Therefore, the quadratic dispersion is a unique signature of the projected SO(5) symmetry in the entire range of densities $0 < \rho < \rho_c$. To understand the physical origin of this remarkable phenomenon, we notice that a boson system with gapless quadratic dispersion generally has infinite compressibility. This can be directly seen from the compressibility sum rule

$$\kappa \equiv \frac{\partial \rho}{\partial \mu} = \frac{1}{2} \lim_{k \rightarrow 0} \lim_{\omega \rightarrow 0} \chi(k, \omega) \sim \lim_{k \rightarrow 0} \frac{k^2}{\omega^2(k)}, \quad (6.11)$$

where $\chi(k, \omega)$ is the dynamical density correlation function. Because of the quadratic dispersion relation, we can see explicitly that $\chi(k) \propto 1/k^2$ for small k ; therefore, a infinite compressibility is obtained. On the other hand, a infinite compressibility implies that $\partial \mu / \partial \rho = 0$, i.e., the chemical potential is independent of doping. But this is exactly the prediction of the projected SO(5) model. For $0 < \rho < \rho_c$, the chemical potential is pinned at the SO(5) symmetric point $\mu = \mu_c$, where the superspin vector can point in any direction. To accommodate a long-wavelength fluctuation of the hole density, the system rotates into another degenerate minimum with a different superspin angle α and a different hole density. For this reason, the chemical potential does not change and the system is infinitely compressible.

VII. QUANTUM CORRECTIONS TO THE MEAN-FIELD SOLUTION

At the mean-field level, the ground-state energy of the Hamiltonian (2.11) with Eq. (6.2) depends on the AF and SC order parameters x and y only via their combination $r^2 = x^2 + y^2$ reflecting the SO(5) invariance of the mean-field result. However, the zero-point energy of the bosons in the quadratic Hamiltonian gives a correction to the ground-state energy due to quantum fluctuations. [Calculations of the quantum fluctuation effects at the SO(3) spin-flop transition have been studied in Ref. 31.] As we will show below, this cor-

rection turns out to depend on x^2 and y^2 separately.

For the soft-constraint case, E_1 can be expressed as

$$E_1 = \frac{1}{2} \sum_k \sum_i \omega_i(k) - 2(\Delta + 2Wr^2), \quad (7.1)$$

where $\omega_i(k)$ are the four collective modes described in Sec. VI (although extended to all values of k in the Brillouin zone). In a systematic $1/s$ expansion, this correction to the ground-state energy scales like $1/s$, and is therefore small in the semiclassical limit. Alternatively, E_1 can be seen as a small correction to the mean-field energy E_0 for small values of the parameter $\epsilon \equiv r^2 W/2J = 1 - \Delta/4J$. However, contrary to E_0 , E_1 also depends on the superspin angle α and thus produces a small SO(5)-symmetry breaking.

We now evaluate the α -dependent part of Eq. (7.1) in the small- ϵ limit. We thus parametrize $\chi = 1 - 2 \sin^2 \alpha$ ($-1 \leq \chi \leq 1$), differentiate the expression (7.1) with respect to χ , and expand it up to second order in ϵ . By further transforming $(\cos k_x + \cos k_y)/2 = 1 - q$ with $0 \leq q \leq 2$, the derivative of E_1 can be expressed as the sum of two terms

$$\frac{d}{d\chi} E_1 = E'_{1A} + E'_{1B}, \quad (7.2)$$

where

$$\frac{E'_{1A}}{E'_{1B}} = 2J \int_0^2 dq \mathcal{D}(q) \frac{G_A}{G_B}, \quad (7.3)$$

with

$$G_A \equiv \frac{[(1 - \sqrt{q}) \epsilon]}{2 \sqrt{q}} + O(\epsilon^2), \quad (7.4)$$

$$G_B \equiv -\frac{(\sqrt{q} - 1)(\chi \sqrt{q} - 1 - \chi - \sqrt{q}) \epsilon^2}{4(1 + \sqrt{q}) q^{3/2}} + O(\epsilon^3), \quad (7.5)$$

and the density of states $\mathcal{D}(q)$ is defined as

$$\mathcal{D}(q) = \frac{1}{4\pi^2} \int dk_x dk_y \delta[q - 1 + (\cos k_x + \cos k_y)/2]. \quad (7.6)$$

Unfortunately, the terms of the ϵ expansion in G_B diverge when integrated over q . It is thus convenient to carry out the transformation $q = \epsilon z$ in G_B and then expand in powers of ϵ . We obtain

$$G_B = \frac{\sqrt{\epsilon}}{2} \left(\frac{1}{\sqrt{z+1+\chi}} - \frac{1}{\sqrt{z}} \right) + O(\epsilon). \quad (7.7)$$

For small ϵ , the integral in z can be extended to ∞ and we obtain from Eq. (7.3)

$$E'_{1B} = 2J \epsilon \int_0^\infty dz \mathcal{D}(z\epsilon) G_B$$

$$= \frac{-(\sqrt{1+\chi}) \epsilon^{3/2}}{\pi} + O(\epsilon^2 \ln \epsilon). \quad (7.8)$$

While in evaluating Eq. (7.8) we only need the density of states at $q=0$, $\mathcal{D}(0) = \pi^{-1}$, for the first term E'_{1A} one needs $\mathcal{D}(q)$ in the whole domain $0 \leq q \leq 2$. However, E'_{1A} is independent of χ and thus it merely fixes the value of the critical chemical potential. A numerical integration yields

$$E'_{1A} = 0.28 J \epsilon. \quad (7.9)$$

By integrating over χ Eqs. (7.9) and (7.8), we finally obtain the total contribution to the ground-state energy correction:

$$\frac{E_1}{2J} = 0.14 \chi \epsilon - \frac{2}{3\pi} [\epsilon(1 + \chi)]^{3/2} + O(\epsilon^2 \ln \epsilon) + \text{const.} \quad (7.10)$$

E_1 thus lifts the degeneracy as a function of χ and initially favors the pure superconducting phase ($\chi = -1$). A small chemical potential term $-\mu' y^2 = -\mu' r^2(1 - \chi)/2$ with $\mu' r^2/2J = \mu'_c r^2/2J = -0.28\epsilon + (2/3\pi)(2\epsilon)^{3/2}$ restores the degeneracy between the pure superconducting ($\chi = -1$) and the pure antiferromagnetic ($\chi = +1$) phases. However, due to the convexity of E_1 as a function of χ there is always a barrier ($\propto J\epsilon^{3/2}$) between the two phases since the mixed phase always has a higher energy. This means that at $\mu' = \mu'_c$ and for intermediate densities the system prefers to phase separate between the two pure phases rather than choosing the mixed phase. However, the important point is that this barrier remains small in the limit $U \rightarrow \infty$.

In view of the symmetry breaking effects of the quantum fluctuations, it would be interesting to see whether there is a limit when the wave function (4.1) and the projected SO(5) symmetry become exact. Rokhsar and Kotliar³² have shown that these types of wave function are actually exact in the limit of infinite dimensions. Therefore, besides the $1/s$ expansion, we could also use a $1/d$ expansion (where d is the space dimension) to systematically control the SO(5) symmetry breaking quantum effects. Besides quantum fluctuations, there are also other symmetry breaking terms. Nearest-neighbor and next-nearest-neighbor Coulomb interactions also break the SO(5) symmetry, however, their corrections to the ground state are concave, i.e., the energy of the intermediate states are lowered. Therefore, they can also lead to uniform mixed states in some region of the phase diagram. The detailed study of all these competing effects will be carried out in subsequent works.

VIII. LOW-ENERGY EFFECTIVE LAGRANGIAN

While the projected SO(5) model defined on a lattice enables us to make some connection to the underlying microscopic physics, for most discussions concerning the long-wavelength and low-energy degrees of freedom, it is desirable to have an effective continuum Lagrangian. Such a formulation can be directly obtained by taking the long-wavelength limit of the projected bosonic model discussed previously. However, in order to make the connection to the unprojected SO(5) model clearer, we shall motivate our discussion from the original SO(5) effective model.

The effective Lagrangian for a fully SO(5) symmetric model takes the form of

$$\mathcal{L} = \frac{\chi}{2}(\partial_t n_a)^2 - \frac{\rho}{2}(\partial_k n_a)^2 - V(n), \quad (8.1)$$

where χ measures the superspin susceptibility, ρ measures the superspin stiffness, $k=x,y$ denotes the spatial directions, and $V(n)$ is a scalar function of the superspin magnitude n_a^2 only. There are three important symmetry breaking effects connected with the presence of a large Mott-Hubbard gap. First is an asymmetry in the scalar potential, which can be described by a additional term

$$V_g(n) = + \frac{g}{2}(n_1^2 + n_5^2), \quad (8.2)$$

which for positive g favors AF at half-filling. Second is the asymmetry between the spin (χ_s) and the charge (χ_c) susceptibilities, which modifies the kinetic energy to

$$\frac{\chi_s}{2}(\partial_t n_\alpha)^2 + \frac{\chi_c}{2}(\partial_t n_i)^2. \quad (8.3)$$

The last symmetry breaking effect is due to the chemical potential μ , which enters the Lagrangian as a gauge coupling in the time direction, and modifies the charge part of the kinetic energy to

$$\frac{\chi_c}{2}[(\partial_t n_1 + \mu n_5)^2 + (\partial_t n_5 - \mu n_1)^2]. \quad (8.4)$$

Combining these three symmetry breaking terms, we obtain

$$\begin{aligned} \mathcal{L} &= \frac{\chi_s}{2}(\partial_t n_\alpha)^2 + \frac{\chi_c}{2}[(\partial_t n_1 + \mu n_5)^2 + (\partial_t n_5 - \mu n_1)^2] \\ &\quad - \frac{\rho}{2}(\partial_k n_a)^2 - V(n) - \frac{g}{2}n_i^2 \\ &= \frac{\chi_s}{2}(\partial_t n_\alpha)^2 + \frac{\chi_c}{2}(\partial_t n_i)^2 + \mu\chi_c(n_5\partial_t n_1 - n_1\partial_t n_5) \\ &\quad + \frac{\mu^2\chi_c - g}{2}n_i^2 - \frac{\rho}{2}(\partial_k n_a)^2 - V(n). \end{aligned} \quad (8.5)$$

In the presence of a large Mott-Hubbard gap, all these three symmetry breaking terms are of the order of U , i.e., $\chi_c^{-1} \sim g \sim \mu_c \sim U$. Therefore, this Lagrangian contains high-energy degrees of freedom of the order of U . However, as already observed in Ref. 1, at $\mu = \mu_c = \sqrt{g/\chi_c}$, their effects cancel completely in the time-independent part of the Lagrangian, and the static potential is SO(5) symmetric just as in the original unprojected model. We also observe that near the AF/SC transition point where $\mu \sim \mu_c$, the first-order time derivative term is of the order of 1. Furthermore, in the spirit of the low-frequency and wave-vector expansion, we only need to retain the first-order time derivative term in the charge sector and can drop the second term in the above Lagrangian. Combining all these considerations, we obtain the following low-energy effective Lagrangian near the AF/SC transition region, which is free of any parameters of the order of U :

$$\mathcal{L} = \frac{\chi_s}{2}(\partial_t n_\alpha)^2 + (n_5\partial_t n_1 - n_1\partial_t n_5) - \frac{\rho}{2}(\partial_k n_a)^2 - V(n). \quad (8.6)$$

This is exactly the Lagrangian counterpart of the SO(5) projection procedure discussed previously in the Hamiltonian language. Dropping the second-order time derivative terms removes half of the (high-energy) degrees of freedom, and redefines the canonical conjugacy of the dynamical variables. In particular, the conjugate variable of n_1 is nothing but n_5 itself, since $p_1 = \delta\mathcal{L}/\delta\partial_t n_1 = 2n_5$. Standard quantization procedure requires the canonical commutation relation $[n_1, p_1] = i$, which in this case just reproduces Eq. (1.4). This confirms the fact that the SO(5) projection does not change the form of the interaction potential, only the commutation relation between n_1 and n_5 .

It is easy to see that the low-energy effective Lagrangian (8.6) produces exactly the same long-wavelength collective mode spectrum as the projected SO(5) Hamiltonian (2.11) defined on a lattice. To facilitate the comparison, we take the SO(5) potential to be

$$V(n) = -\frac{\delta}{2} \sum_a n_a^2 + \frac{W}{4} n_a^4, \quad \delta > 0. \quad (8.7)$$

Assuming broken symmetry in the n_1 and n_2 directions, we find that the n_3 and n_4 modes always decouple, and they have a linear spin-wave dispersion relation with $v_s = \sqrt{\rho/\chi_s}$. The Euler-Lagrangian equations of motion gives the following dispersion relation for the n_1 and n_2 modes:

$$\omega^2 = \begin{cases} \frac{1}{4}\rho^2 k^4 \\ \frac{\rho}{\chi_s} k^2 + \frac{2\delta}{\chi_s} \end{cases} \quad (8.8)$$

for the AF state with $\langle n_1 \rangle = 0, \langle n_2 \rangle \neq 0$,

$$\omega^2 = \begin{cases} \frac{1}{2}\rho\delta k^2 \\ \frac{\rho}{\chi_s} k^2 \end{cases} \quad (8.9)$$

for the SC state with $\langle n_1 \rangle \neq 0, \langle n_2 \rangle = 0$, and

$$\omega^2 = \begin{cases} \frac{1}{4}(1 + \sin^2 \alpha \cos^2 \alpha)\rho^2 k^4 \\ \frac{2\delta \cos^2 \alpha}{\chi_s} + \left(\frac{1}{2}\delta\rho \sin^2 \alpha + \frac{\rho}{\chi_s} \right) k^2 \end{cases} \quad (8.10)$$

for the mixed state with $\langle n_1^2 \rangle = (\delta/W)\sin^2 \alpha$ and $\langle n_2^2 \rangle = (\delta/W)\cos^2 \alpha$. These dispersion relations agree exactly with the lattice model results at the projected SO(5) symmetric point if we make the following identification:

$$\rho = 2J, \quad \chi_s = \frac{1}{2J}, \quad \delta = 2(4J - \Delta). \quad (8.11)$$

The effective Lagrangian can be easily used to discuss effects of SO(5) symmetry breaking. The simplest form of symmetry breaking is increasing the chemical potential be-

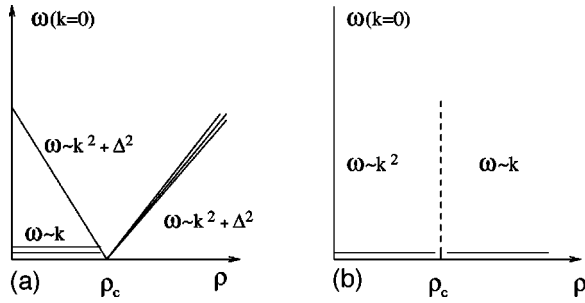


FIG. 5. Evolution of the collective mode spectra as a function of density in the projected SO(5) model. (a) shows the gap towards spin excitations. Charge excitations are gapless for the entire region of density, however, the dispersion relation changes from $\omega \sim k^2$ to $\omega \sim k$ at ρ_c , as indicated in (b).

yond the critical value μ_c , so that a pure SC state is realized. The chemical potential enters the effective Lagrangian through the gauge coupling in the time direction via the following substitution:

$$\partial_t n_1 \Rightarrow \partial_t n_1 + \delta\mu n_5, \quad \partial_t n_5 \Rightarrow \partial_t n_5 - \delta\mu n_5, \quad (8.12)$$

where $\delta\mu \equiv \mu - \mu_c$ is the deviation of the chemical potential away from the critical value. In this case, the spin-triplet excitations acquire a finite mass gap, with the following dispersion relation:

$$\omega^2(k) = \frac{\rho k^2}{\chi_s} + \frac{4(\mu - \mu_c)}{\chi_s} \quad (8.13)$$

and the mass gap increases with increasing doping in the SC state.

We summarize the behavior of the collective modes obtained in the previous two sections in Fig. 5. We see that while there are significant modifications of the collective mode spectra in the density regime $0 < \rho < \rho_c$ from the unprojected SO(5) symmetry, the spectra beyond ρ_c is essentially identical to the behavior expected from the unprojected SO(5) symmetry. This should be expected from our general considerations about the Gutzwiller projection without much detailed calculations. We argued that the only effect of the Gutzwiller projection is to change the quantum commutation relation between the SC components of the superspin n_1 and n_5 . However, for $\rho > \rho_c$, the system is in a pure SC phase where these components acquire classical expectation values. In this case, the modification of the quantum commutation relation does not have any significant effect. This argument can also be illustrated by a simple picture of a *chiral* SO(5) sphere, as depicted in Fig. 6.

In this picture, the north and south poles represent the three AF directions, and the equatorial plane represents the SC directions. The sphere is perfectly SO(5) symmetric. However, the chemical potential along the pole direction acts like a fictitious magnetic field which restricts the sense of the rotation in the SC plane. Small oscillations of a vector pointing close to the north pole enclose the fictitious magnetic flux, and can only execute chiral rotations. This amounts to the projection of the particle-pair states at half-filling. On the other hand, small oscillations of a vector pointing anywhere along the equator does not enclose the fictitious magnetic flux, and their dynamics is therefore unaffected by the pro-

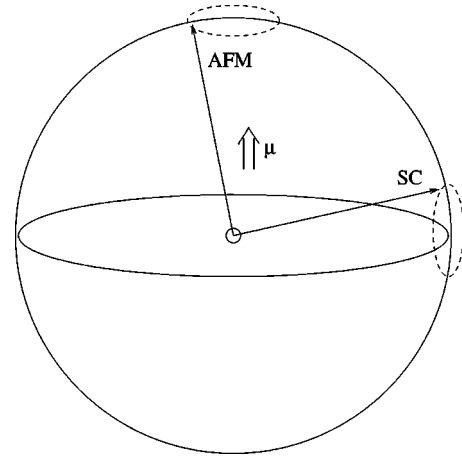


FIG. 6. Pictorial representation of a chiral SO(5) sphere.

jection. Dynamics of a vector pointing anywhere between the north pole and the equator is also partially affected by the projection, but the symmetry of the static potential bears a unique signature.

IX. CONCLUSION

The main purpose of this paper is to introduce the concept of projected SO(5) models and discuss the properties of this model in connection with high- T_c superconductivity. The projected SO(5) model describes the low-energy and long-distance bosonic degrees of the freedom near the AF/SC transition. We showed that the Gutzwiller projection can be implemented analytically on every site in the SO(5) theory. In the presence of a infinite Mott-Hubbard gap, we show that static properties of the model can remain SO(5) symmetric, while the modification of the dynamics can be completely cast into a nontrivial commutation relation between the two SC components of the SO(5) superspin. Unlike the unprojected SO(5) models which can only have the full dynamic SO(5) symmetry at half-filling, the projected SO(5) model can have static SO(5) symmetry at a critical value of the chemical potential μ_c and for a finite range of doping $0 \leq \rho \leq \rho_c$. At $\rho = 0$, the system has an AF ground state and zero compressibility. In the intermediate regime $0 < \rho < \rho_c$, the system has mixed AF and SC order and infinite compressibility. For $\rho > \rho_c$, the system has a pure SC ground state; the SC order parameter rises to a maximal value before it decreases with doping. At the projected SO(5) symmetric point, we can understand precisely the evolution of the collective modes. On the AF side, we have two gapless spin-wave modes and a gapless charge mode describing the gapless fluctuation from AF to SC. In the intermediate density regime $0 < \rho < \rho_c$, the physical properties of the spin waves remain unchanged, while the massive spin amplitude mode gradually decreases its energy and merges with the two spin-wave modes at $\rho = \rho_c$. The charge mode in the intermediate density regime is gapless, but has a quadratic dispersion relation, which is a unique signature of the projected SO(5) symmetry. For $\rho > \rho_c$, the charge mode is gapless with a linear dispersion relation, and the π triplet spin mode becomes massive, and gradually increases its energy with increasing doping. In this regime, the behavior of the collective modes are identical to the unprojected SO(5) model.

This very simple model can form the basis for under-

standing many puzzling properties of the high- T_c superconductors in a unified framework. It points out a route from AF to SC through a gradual rotation of the superspin angle. At the projected SO(5) symmetry point the mean-field energy is independent of the superspin angle, and therefore it offers an explanation of the absence of the chemical potential shift in the underdoped regime without global phase separation. It predicts a phase diagram which is qualitatively consistent with the observed phase diagram in the high- T_c materials. In the underdoped regime of the phase diagram, the systems have large AF and SC fluctuations, and these fluctuations can be responsible for the pseudogap physics observed in these materials.

There are many possible directions to carry out this line of research in the future. The most important issue is to understand the precise nature of the intermediate state in the regime $0 < \rho < \rho_c$. Since the system has infinite compressibility in this regime, different small perturbation may select different ground states. Such perturbing effects might include quantum fluctuations and longer ranged interactions. In particular, we would like to investigate the possibility that these perturbations might lead to the formation of incommensurate order or stripes.

In this work, we have discussed extensively the collective fluctuations in the long-wavelength limit. Due to the definitions of our effective lattice model, the $k \rightarrow 0$ limit corresponds to the $k \rightarrow 0$ limit in the SC correlation functions and the $k \rightarrow (\pi, \pi)$ limit of the AF spin correlation functions. Within the SO(5) theory, the π resonance in the SC state is viewed as the SO(5) symmetry partner of the $k \rightarrow 0$ Goldstone mode of the SC phase fluctuation. While the commensurate neutron resonance mode is observed in both Y-Ba-Cu-O and Bi-Sr-Ca-Cu-O superconductors, all high- T_c systems also have incommensurate spin fluctuations. How can these features be explained within the current theoretical model?

The fact that La-Sr-Cu-O and Y-Ba-Cu-O have very different Fermi surface shapes and yet have similar incommensurate magnetic peaks strongly suggests that the incommensurate peaks are not sensitive to Fermi surface effects and should be explainable within an effective bosonic model. Let us recall that the collective mode of a superfluid boson system consists of a linearly dispersing phonon branch and another roton branch with a minimum located at the inverse interparticle spacing. So far, we have only studied the phonon branch of the charged bosons. By analogy, the roton branch should also exist, with a wave vector determined by the density of the charged bosons or doping. Within the SO(5) theory, while the commensurate neutron resonance can be viewed as the SO(5) partner of the SC phase mode, the incommensurate magnetic peaks can be viewed as the SO(5) partner of the roton minimum of the charged bosons. A detailed quantitative analysis of this picture will be carried out in the future.

However, while the ground state in the doping range $0 < \rho < \rho_c$ may depend sensitively on small perturbation effects, at finite temperature, these perturbation effects should be small and the system should display more universal properties. We have shown that the projected SO(5) symmetry should be valid for the entire doping range $0 < \rho < \rho_c$, and we shall quantitatively study the manifestation of this sym-

metry at finite temperature, and see if the projected SO(5) symmetry can give a universal explanation of the pseudogap physics.

Note added in proof. After completing this work, we received a very interesting paper by Coen van Duin,³⁵ in which he also observed the remnant SO(5) behavior in the large U limit.

ACKNOWLEDGMENTS

We would like to acknowledge useful discussions with D. Arovas, J. Berlinsky, E. Demler, R. Eder, C. Kallin, S. Kivelson, and D. Scalapino. S.C.Z. and J.P.H. were supported by the NSF under Grant No. DMR-9814289. W.H. and E.A. were supported by FORSUPRA II, BMBF (05 605 WWA 6), the Deutsche Forschungsgemeinschaft (AR 324/1-1) and (HA 1537/17-1), and A.A. by the Israel Science Foundation. A.A., E.A., and W.H. would like to acknowledge the support and hospitality of the Stanford Physics Department, where most of this work was carried out.

APPENDIX: SLAVE BOSON RESULTS

Alternatively, one can enforce the hard-core constraint (6.1) by introducing an additional ‘‘slave’’ boson for each lattice site. The presence of this boson [$e(x)$] indicates that the lattice site x is in the singlet state. The ‘‘less or equal’’ hard-core condition (6.1) is replaced with the equality constraint

$$Q(x) = \sum_{\alpha} t_{\alpha}^{\dagger}(x)t_{\alpha}(x) + t_h^{\dagger}(x)t_h(x) + e^{\dagger}(x)e(x) - q = 0, \quad (\text{A1})$$

with $q=1$. Since in physical states one always has one and only one boson per lattice sites, destruction (creation) of a boson t_a (t_a^{\dagger}) must always be accompanied by creation (destruction) of the empty boson e^{\dagger} (e). In this way, the *physical* operators for creating (destroying) a triplet ($a=x, y, z$) or a hole pair ($a=h$) acquire the form $t_a^{\dagger}e$ ($t_a e^{\dagger}$). The advantage of this method is that the constraint can be enforced exactly (at least in principle) by introducing an additional time-independent field $\lambda(x)$ at each lattice site, by adding to the Hamiltonian a term $-\lambda(x)Q(x)$ and by integrating over the $\lambda(x)$ on the imaginary axis. The whole Hamiltonian (2.11) thus takes the form (apart from a constant)

$$\begin{aligned} H_{sb} = & - \sum_x \lambda(x)Q(x) + \Delta_s \sum_{x,\alpha} t_{\alpha}^{\dagger}(x)t_{\alpha}(x) \\ & + \tilde{\Delta}_c \sum_x t_h^{\dagger}(x)t_h(x) - J_s/2 \sum_{\langle x,x' \rangle, \alpha} [t_{\alpha}^{\dagger}(x)e(x) + \text{H.c.}] \\ & \times [t_{\alpha}^{\dagger}(x')e(x') + \text{H.c.}] \\ & - J_c/2 \sum_{\langle x,x' \rangle} [t_h^{\dagger}(x)e(x)e^{\dagger}(x')t_{\alpha}(x')e(x') + \text{H.c.}] \end{aligned} \quad (\text{A2})$$

In practice, one starts with a mean-field approximation and expands the boson operators around their mean-field values as in Sec. VI. This expansion can be rigorously con-

trolled by generalizing the constraint (A1) to large values of q , whereby one scales $J_{c/s} \rightarrow J_{c/s}/s$ (cf. Refs. 33 and 34). Physically, this corresponds to allowing for a large number of bosons to be present at each site and thus to have a large value for the total spin, or more precisely for the SO(5) quantum number s , at each site. The mean-field result thus corresponds to the $q \rightarrow \infty$ limit, while the quadratic expansion corresponds to the first $1/q$ correction.

At the mean-field level, the constraint is fulfilled exactly and indeed one obtains the same result and the same phase diagram as the variational ansatz (4.1) discussed in Sec. V. By expanding the bosons quadratically around the mean field one obtains the same modes as for the soft-core Hamiltonian with a similar dispersion. [Here, we restrict ourselves again to the SO(5)-symmetric case.] Specifically, in the mixed phase one obtains two spin-wave modes with dispersion

$$\omega(k) = \frac{4J + \Delta}{4} k, \quad (\text{A3})$$

one massive spin-amplitude mode

$$\omega(k)^2 = (16J^2 - \Delta^2) \cos^2 \alpha + O(k^2), \quad (\text{A4})$$

and a quadratic mode

$$\omega(k) = \frac{4J + \Delta}{8 \cos \alpha} k^4. \quad (\text{A5})$$

In the pure superconducting phase, one has a π -triplet with dispersion

$$\omega(k) = \frac{4J + \Delta}{4} k \quad (\text{A6})$$

and the SC Goldstone mode with dispersion

$$\omega(k)^2 = \frac{16J^2 - \Delta^2}{4} k^2. \quad (\text{A7})$$

These results coincide with the ones of the soft-constraint approximation Eqs. (6.6)–(6.10) in the limit of small $4J - \Delta$, i.e., for low boson density.

-
- ¹Shou-Cheng Zhang, *Science* **275**, 1089 (1997).
²C. Henley, *Phys. Rev. Lett.* **80**, 3590 (1998).
³S. Rabello, H. Kohno, E. Demler, and S.C. Zhang, *Phys. Rev. Lett.* **80**, 3586 (1998).
⁴C. Burgess, J. Cline, R. MacKenzie, and R. Ray, *Phys. Rev. B* **57**, 8549 (1998).
⁵D. Scalapino, S.C. Zhang, and W. Hanke, *Phys. Rev. B* **58**, 443 (1998).
⁶R. Eder *et al.*, *Phys. Rev. B* **59**, 561 (1999).
⁷S. Meixner, W. Hanke, E. Demler, and S.-C. Zhang, *Phys. Rev. Lett.* **79**, 4902 (1997).
⁸R. Eder, W. Hanke, and S.C. Zhang, *Phys. Rev. B* **57**, 13 781 (1998).
⁹W. Hanke *et al.*, cond-mat/9807015 (unpublished).
¹⁰A. Auerbach, cond-mat/9801294 (unpublished).
¹¹C. Burgess and A. Lutken, *Phys. Rev. B* **57**, 8642 (1998).
¹²Xiao Hu, Tomio Koyama, and Masashi Tachiki, *Phys. Rev. Lett.* **82**, 2568 (1999).
¹³E. Demler and Shou-Cheng Zhang, *Phys. Rev. Lett.* **75**, 4126 (1995).
¹⁴E. Demler, H. Kohno, and S.-C. Zhang, *Phys. Rev. B* **58**, 5719 (1998).
¹⁵Y. Bazaliy, E. Demler, and S.-C. Zhang, *Phys. Rev. Lett.* **79**, 1921 (1997).
¹⁶D. Arovas, A.J. Berlinsky, C. Kallin, and S.C. Zhang, *Phys. Rev. Lett.* **79**, 2871 (1997).
¹⁷E. Demler, A.J. Berlinsky, C. Kallin, G. Arnold, and M. Beasley, *Phys. Rev. Lett.* **80**, 2917 (1998).
¹⁸D. Sheehy and P. Goldbart, *Phys. Rev. B* **57**, 8131 (1998).
¹⁹P.M. Goldbart and D. Sheehy, *Phys. Rev. B* **58**, 5731 (1998).
²⁰M. Greiter, *Phys. Rev. Lett.* **79**, 4898 (1997).
²¹S. Meixner, W. Hanke, E. Demler, and S.-C. Zhang, *Phys. Rev. Lett.* **79**, 4937 (1997).
²²G. Baskaran and P.W. Anderson, *J. Phys. Chem. Solids* **59**, 1780 (1998).
²³Shou-Cheng Zhang, *J. Phys. Chem. Solids* **59**, 1774 (1998).
²⁴R. Prange and S.M. Girvin, *The Quantum Hall Effect* (Springer-Verlag, Berlin, 1997).
²⁵R. Eder, *Phys. Rev. B* **59**, 13 810 (1999).
²⁶A. Ino, T. Mizokawa, and A. Fujimori, *Phys. Rev. Lett.* **79**, 2101 (1997).
²⁷F.F. Assaad and M. Imada, *Phys. Rev. Lett.* **76**, 3176 (1996).
²⁸J. Zaanen, cond-mat/9711009 (unpublished).
²⁹V.J. Emery and S. Kivelson, cond-mat/9809083 (unpublished).
³⁰S.R. White and D.J. Scalapino, *Phys. Rev. Lett.* **80**, 1272 (1998).
³¹Ehud Altman and A. Auerbach (unpublished).
³²D. Rokhsar and B.G. Kotliar, *Phys. Rev. B* **44**, 10 328 (1991).
³³N. Read and D. Newns, *J. Phys. C* **16**, 3273 (1983).
³⁴E. Arrigoni, C. Castellani, M. Grilli, R. Raimondi, and G.C. Strinati, *Phys. Rep.* **241**, 291 (1994).
³⁵Coen N.A. van Duin, Ph.D. thesis, University of Leiden, 1999.